PHYSICAL REVIEW B **96**, 121118(R) (2017)

Investigation of the chiral antiferromagnetic Heisenberg model using projected entangled pair states

Didier Poilblanc
Laboratoire de Physique Théorique, CNRS and Université de Toulouse, 31062 Toulouse, France
(Received 27 July 2017; published 27 September 2017)

A simple spin-$\frac{1}{2}$ frustrated antiferromagnetic Heisenberg model (AFHM) on the square lattice—including chiral plaquette cyclic terms—was argued [A. E. B. Nielsen, G. Sierra, and J. I. Cirac, Nat. Commun. **4**, 2864 (2013)] to host a bosonic Kalmeyer-Laughlin (KL) fractional quantum Hall ground state [V. Kalmeyer and R. B. Laughlin, Phys. Rev. Lett. **59**, 2095 (1987)]. Here, we construct generic families of chiral projected entangled pair states (chiral PEPS) with low bond dimension ($D = 3,4,5$) which, upon optimization, provide better variational energies than the KL *Ansatz*. The optimal $D = 3$ PEPS exhibits chiral edge modes described by the Wess-Zumino-Witten $SU(2)_1$ model, as expected for the KL spin liquid. However, we find evidence that, in contrast to the KL state, the PEPS spin liquids have power-law dimer-dimer correlations and exhibit a gossamer long-range tail in the spin-spin correlations. We conjecture that these features are genuine to *local* chiral AFHM on bipartite lattices.

DOI: 10.1103/PhysRevB.96.121118

Introduction. Topological order (TO) has been rationalized in the last few decades [1,2] as a new type of order in two dimensions (2D), beyond the well-known Ginzburg-Landau paradigm. Importantly, it is at the heart of the rapidly expanding field of quantum computing [3]. The fractional quantum Hall (FQH) state of the 2D electron gas [4] is the first topological ordered state discovered. The simple Laughlin wave function provides a beautiful qualitative understanding of the physics of the Abelian FQH state at filling fraction $\nu = 1/m$ as an incompressible fluid [5], while more involved wave functions can also describe non-Abelian FQH states [6–8]. It revealed the emergence of fractional excitations, the anyons, a key feature of TO [1]. Anyons carry fractional charge [5] as well as Abelian [9] or non-Abelian statistics [6,10]. An important feature of FQH states is the existence of a bulk gap and chiral modes providing unidirectional transport on the edge [11,12]. More precisely, their edge physics can be described by chiral $SU(2)_k$ Wess-Zumino-Witten (WZW) conformal field theory (CFT) [13]. Recently, a matrix product state (MPS) representation of the FQH states [14,15] enabled one to probe their physical properties with unprecedented numerical accuracy.

In a pioneering work [16], Kalmeyer and Laughlin (KL) have extended the notion of the FQH state to the lattice. When localized on the lattice, the bosonic $\nu = \frac{1}{b}$ Laughlin state gives rise to a spin-$\frac{1}{2}$ chiral spin liquid (CSL) [17], closely related to the resonating valence bond (RVB) state of high-T_c superconductivity [18]. Recently, fractional Chern insulators [19–21] have set up a new route to realize FQH physics on the lattice.

Whether simple local lattice Hamiltonians can host chiral spin liquid ground states [17] is one of the key issues that determine whether or not such topological phases could be realized experimentally. The original innovative proposal by KL that the ground state (GS) of the frustrated triangular spin-$\frac{1}{2}$ antiferromagnetic Heisenberg model (AFHM) is a CSL turned out not to be correct, the GS of this model being magnetically ordered. However, Bauer *et al.* [23] showed recently that, on the kagome lattice (2D lattice of corner-sharing triangles), the GS of the Hamiltonian $H = \sum_{\triangle(ijk)} \mathbf{S}_i \cdot (\mathbf{S}_\mathbf{j} \times \mathbf{S}_\mathbf{k})$, the sum of the chiral spin interaction over all triangles $\triangle(ijk)$, has the universal properties of the $\nu = \frac{1}{2}$ Laughlin state. This CSL was shown to be exceptionally robust under the addition of an extra nearest-neighbor Heisenberg-like interaction (defining a generic "chiral AFHM"), even of large magnitude.

Another alternative approach has been pursued, trying to construct "parent Hamiltonians" for the Abelian [24,25] and non-Abelian [26,27] CSL. Using a rewriting of the wave function as a correlator of a $1+1$ chiral CFT [28,29], the simplest spin-$\frac{1}{2}$ parent Hamiltonian on the square lattice obtained by Nielsen *et al.* [22] consists of interactions between all pairs and triplets of spins in the system. Since long-range interactions might be hard to achieve experimentally in, e.g., cold atom systems [30], the authors argue that a similar (Abelian) CSL phase is also hosted in a simplified *local* Hamiltonian where all the long-range parts of the interaction have been set to zero [22]. We shall adopt here their local chiral AFHM which, introducing a slightly different parametrization, reads

$$H = J_1 \sum_{\langle i,j \rangle} \mathbf{S}_i \cdot \mathbf{S}_j + J_2 \sum_{\langle\langle k,l \rangle\rangle} \mathbf{S}_k \cdot \mathbf{S}_l + \lambda_c \sum_{\square(ijkl)} i\left(P_{ijkl} - P_{ijkl}^{-1}\right), \quad (1)$$

where the first (second) sum is taken over nearest-neighbor (next-nearest-neighbor) bonds and the last sum over all plaquettes of the square lattice. P_{ijkl} makes a cyclic permutation of the four spins of every plaquette in, e.g., the clockwise direction. H breaks time reversal symmetry but preserves the global spin SU(2) symmetry. It is the analog for the square lattice of the chiral AFHM on the kagome lattice studied by Bauer *et al.* [23]: The chiral interaction $\mathbf{S}_i \cdot (\mathbf{S}_\mathbf{j} \times \mathbf{S}_\mathbf{k})$ on the triangle is replaced here by its generalization on the plaquette and magnetic frustration is introduced via competing J_1 and J_2 antiferromagnetic couplings. A schematic phase diagram showing the (approximate) extension of the KL chiral spin liquid is provided for convenience in Fig. 1. We shall here focus on the two special points studied by Nielsen *et al.* [22] and located in Fig. 1, supposedly in the CSL phase: $J_1 = 2$, $J_2 = 0$, $\lambda_c = 1$, and $J_1 = 2\cos(0.06\pi)\cos(0.14\pi) \simeq 1.78$, $J_2 = 2\cos(0.06\pi)\sin(0.14\pi) \simeq 0.84$, $\lambda_c = 2\sin(0.06\pi) \simeq 0.375$. Hereafter, we refer to the latter as the "J_1-λ_c model" and the "J_1-J_2-λ_c model," respectively.

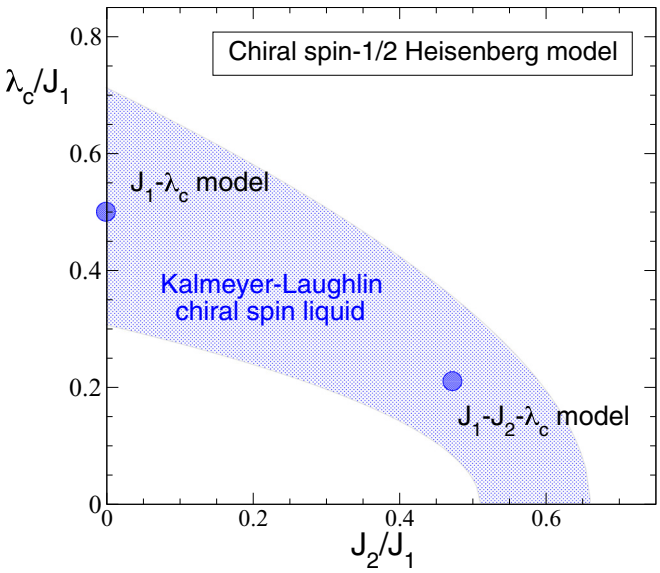

FIG. 1. Schematic phase diagram of the chiral AFHM drawn from Ref. [22] as a function of magnetic frustration J_2/J_1 and (relative) amplitude of the chiral interaction λ_c/J_1. The KL nature and the boundary of the chiral spin liquid phase (blue region) was only accessed from small cluster calculations. The location in parameter space of the two models studied here are shown by (blue) dots.

Our strategy to explore the physics of the above model is to use the tensor network framework [31–35]. One of the motivations is to test whether some fundamental obstruction is at play that prevents one to describe a gapped CSL phase with 2D tensor networks [36]. Previous attempts using projected entangled pair states (PEPS) led to the discovery of *critical* CSL exhibiting chiral edge modes [37–39]. PEPS are *Ansätze* that approximate GS wave functions in terms of a unique site tensor $A^s_{\alpha\beta\gamma\delta}$, where the greek indices label the states of the D-dimensional *virtual* spaces $\mathcal{V}$ attached to each site in the $z = 4$ directions of the lattice, and $s = \pm\frac{1}{2}$ is the S_z component of the physical spin. The site tensors are then entangled together (i.e., contracted with respect to their virtual indices) to form a 2D tensor network. *A priori*, all the $2D^4$ coefficients of the site tensor can serve as parameters to optimize the variational GS energy. However, the CSL bears a number of symmetry properties that greatly constrains the PEPS *Ansatz*. Recently, a classification of fully SU(2)-symmetric (singlet) PEPS was proposed [40] in terms of the irreducible representations (IRREP) of the lattice point group (C_{4v} in the case of the 2D square lattice). Since the CSL should be invariant under the combination of a reflection $\mathcal{R}$ with respect to to any crystalline direction (x, y, $x \pm y$) and time reversal symmetry (i.e., complex conjugation), the simplest adequate PEPS site tensors have the form $A = A_R^{(A_1)} + i A_I^{(A_2)}$, where the two real tensors $A_R^{(A_1)}$ and $A_I^{(A_2)}$ transform according to the A_1 (symmetric with respect to $\mathcal{R}$) and A_2 (antisymmetric with respect to $\mathcal{R}$) IRREP [38,39]. These tensors have been tabulated in Ref. [40] for $D \leqslant 6$, and their numbers for all virtual spaces $\mathcal{V}$ considered in this work are listed in Table I. Following a previous study of the nonchiral frustrated AFHM [41], we consider a general superposition of all tensors of each class, the weights in the sum being considered as variational parameters. As in the nonchiral case, the energy or observables can be computed directly in the thermodynamic limit using infinite-PEPS (iPEPS) corner transfer matrix (CTM) renormalization group (RG) techniques [42–45], making advantage of simplifications introduced by the use of point-group symmetric tensors [41]. At each RG step a truncation of the (Hermitian) CTM is done keeping (at most) χ eigenvalues and preserving exactly the SU(2) multiplet structure. Energy optimization [46–48] is performed using a conjugate gradient (CG) method [49] up to a maximum $\chi = \chi_{\rm opt}$ and then, eventually, one takes the limit $\chi \to \infty$ (using a "rigid" *Ansatz*) by extrapolating the data [41].

TABLE I. Numbers of independent SU(2)-symmetric tensors for the four different virtual spaces we consider, $D \leqslant 5$. The third (fourth) column gives the number of A_1 (A_2) tensors and the last column the total number of tensors in the *A Ansatz*. Note that all four types of *Ansätze* exhibit a gauge-$\mathbb{Z}_2$ symmetry associated with the conserved parity of the number of spin-$\frac{1}{2}$ on the $z = 4$ bonds.

$\mathcal{V}$	D	$A_R^{(A_1)}$	$A_I^{(A_2)}$	Total No.
$\frac{1}{2} \oplus 0$	3	2	1	3
$\frac{1}{2} \oplus 0 \oplus 0$	4	8	4	12
$\frac{1}{2} \oplus \frac{1}{2} \oplus 0$	5	10	8	18
$\frac{1}{2} \oplus 0 \oplus 0 \oplus 0$	5	21	12	33

We now turn to the results. In Fig. 2 we show the scaling of the iPEPS energies versus D^2/χ for the two local chiral Hamiltonians studied here, and different choices of the virtual space $\mathcal{V}$ up to $D \leqslant 5$. Using linear fits, one obtains accurate variational energies in the $\chi \to \infty$ limit, apart from $D = 5$ for which the CTM RG converges to unphysical (pairs of) solutions beyond $\chi = 2D^2$. The exact GS energies obtained on a small periodic 30-site cluster [22] (expected to give a

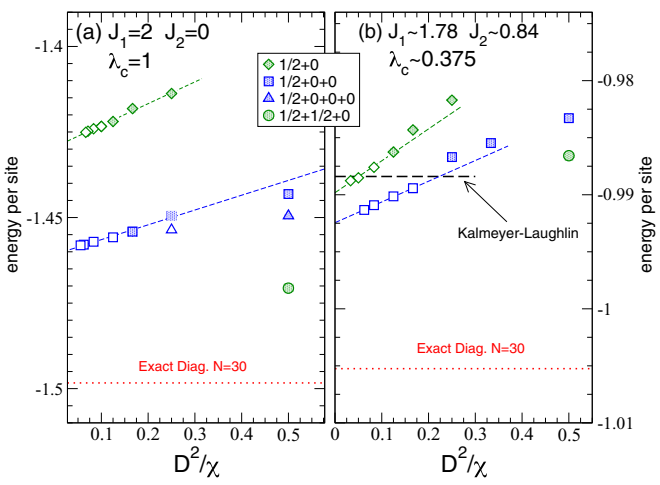

FIG. 2. Scaling of the iPEPS variational energies (per site) vs D^2/χ for the two local chiral Hamiltonians studied here: (a) J_1-λ_c model; (b) J_1-J_2-λ_c model. The solid (open) symbols correspond to fully optimized (fixed) tensors as explained in the text. A comparison with the exact energy (per site) of a 5×6 torus [22] is shown. In (b) the variational energy of the Kalmeyer-Laughlin (KL) spin liquid obtained by Monte Carlo [22] is also shown.

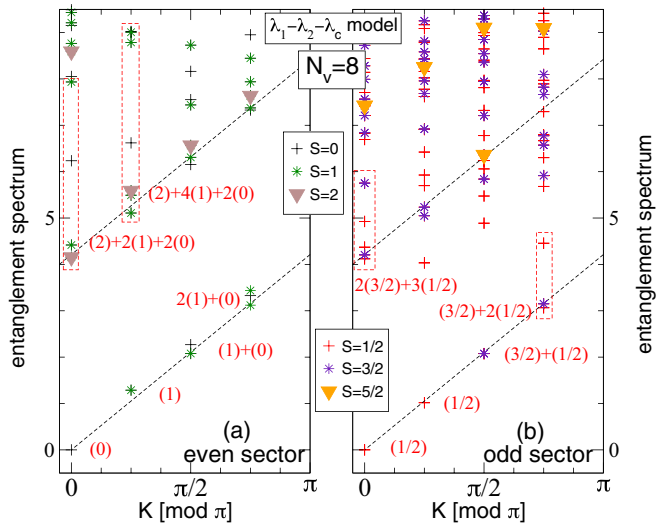

FIG. 3. Chiral entanglement spectra of the $D = 3$ PEPS optimized for the J_1-J_2-λ_c model (subtracting the GS energy for convenience) for $N_v = 8$. The edge momentum K is defined mod-π since the SU(2) generators are invariant under only sublattice translations. (a) Even and (b) odd $\mathbb{Z}_2$ sectors are shown. The correct $SU(2)_1$ counting obtained for each quasidegenerate group of levels at low energy (outlined by boxes when necessary) is indicated in red.

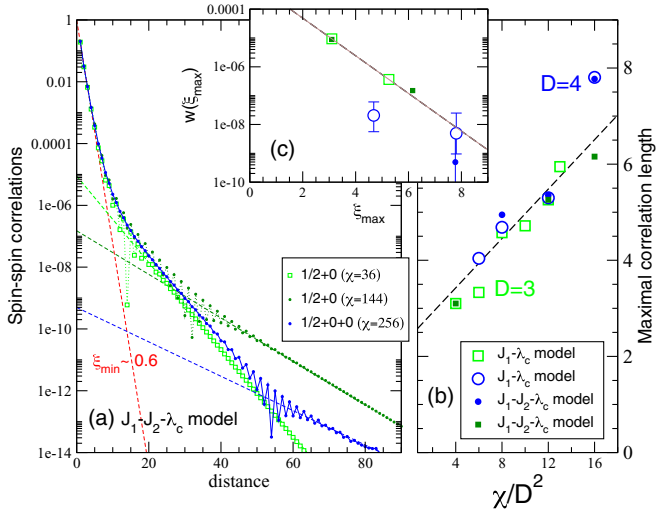

FIG. 4. (a) Absolute value of the spin-spin correlations vs distance (along some crystal axis direction x or y) for the $D = 3$ and $D = 4$ (optimized) chiral PEPS and different environment dimension χ (as shown in legends) on a semilog plot. The dashed lines are fits according to exponential behaviors of the short- and long-distance correlations. (b) Largest correlation length $\xi_{\max}$ [obtained from the linear fits in (a)] vs χ/D^2, for both model parameter sets. (c) $w(\xi_{\max})$ vs $\xi_{\max}$ using the same symbols as in (b).

lower bound of the true thermodynamic values) provide a first reference, showing that the iPEPS energies are remarkably accurate. For the second model in Fig. 2(b), we have compared our results to the variational energy of the KL *Ansatz* computed with Monte Carlo [22]. We find that, even for the smallest bond dimensions $D = 3$ ($\mathcal{V} = \frac{1}{2} \oplus 0$) and $D = 4$ ($\mathcal{V} = \frac{1}{2} \oplus 0 \oplus 0$), the iPEPS energy is lower than the energy of the KL CSL. This provides solid arguments that these chiral SU(2)-invariant PEPS are very good variational states. Hereafter we investigate further their edge and bulk properties and point out similarities and differences with the KL wave function.

Chiral edge modes. First, we have computed the entanglement spectrum (ES) of the optimized $D = 3$ PEPS on an infinitely long cylinder $\mathcal{C}$, bipartitioned into two semi-infinite half cylinders $\mathcal{C}_L$ and $\mathcal{C}_R$, $\mathcal{C} = \mathcal{C}_L \cup \mathcal{C}_R$. This can be done exactly [50] on cylinders with up to $N_v = 8$ sites of circumference. Li and Haldane [51] have conjectured that, in chiral topological states, there is a deep one-to-one correspondence between the true physical edge spectrum and the ES [52,53]. The ES is obtained from the leading eigenvector of the finite-dimensional $D^{2N_v} \times D^{2N_v}$ transfer matrix of the cylinder, as originally proposed in Ref. [50], and already applied to chiral spin liquids [38,39]. The ES shown in Fig. 3 as a function of the momentum K along the cut clearly reveal the existence of well-defined chiral branches linearly dispersing as $E_K \sim vK$. One also sees quasidegenerate groups of levels whose counting [in terms of SU(2) multiplets] matches exactly the one of the $SU(2)_1$ WZW CFT [13], as expected in a KL CSL phase [54]. Note that the ES of the optimized PEPS is remarkably similar to the one obtained for another studied chiral PEPS [38,39], certainly belonging to the same $D = 3$ chiral PEPS family, but far away in parameter space. Although the same exact calculation cannot be realized for $N_v = 8$ beyond $D = 3$, we conjecture that the $SU(2)_1$ chiral edge modes are genuine features of our chiral PEPS optimized for Hamiltonian (1).

Bulk properties. The KL CSL is expected to have short-range (spin-spin) correlations [16] as the bosonic $\nu = \frac{1}{2}$ FQH state it derives from. We investigate now the correlation functions of the PEPS *Ansätze*, and establish important differences. We use the same definitions and CTM RG procedure as described in the study of the frustrated AFHM and focus on the two cases $D = 3$ ($\mathcal{V} = \frac{1}{2} \oplus 0$) and $D = 4$ ($\mathcal{V} = \frac{1}{2} \oplus 0 \oplus 0$). Figure 4(a) shows the spin-spin correlations versus distance on a semilog plot. At short distance, we observe a rapid exponential fall-off characteristic of the KL CSL. However, our data clearly show additional exponential tails with much larger characteristic lengths but with much smaller weights. In other words, we can parametrize the correlation function versus distance as

$$C_S(d) = \sum_{\xi_{\min} \leqslant \xi \leqslant \xi_{\max}} w(\xi) \exp(-d/\xi), \qquad (2)$$

where the short-distance decay is characterized by $w(\xi_{\min}) \simeq 1$ while, at long distance, the slower decay $\exp(-d/\xi_{\max})$ takes over with $\xi_{\max} \gg \xi_{\min}$ and $w(\xi_{\max}) \ll 1$. In fact, we think that $\xi_{\max} \to \infty$ when $\chi \to \infty$ [see Fig. 4(b)] while, simultaneously, $w(\xi_{\max})$ goes very rapidly to zero. If, as suggested in Fig. 4(c), $w(\xi) \propto \exp(-\xi/\lambda)$, where $\lambda \simeq 0.7 \sim \xi_{\min}$, $C_S(d)$ will show a typical stretched exponential form at long distance, $C_S(d) \sim (d/\lambda)^{\frac{1}{4}} \exp\{-(d/\lambda)^{\frac{1}{2}}\}$. In any case, $C_S(d)$ should exhibit a "gossamer tail" which decays slower than any single exponential function.

The dimer-dimer correlations are shown in Fig. 5(a). The asymptotic long-distance behaviors can always be fitted as exponential decays. The correlation lengths extracted from

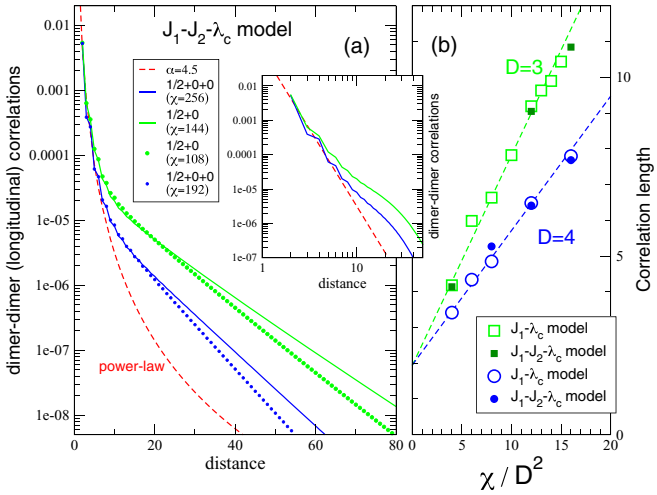

FIG. 5. (a) Absolute value of the dimer-dimer correlations vs distance d (along some crystal axis direction) for the $D = 3$ and $D = 4$ (optimized) chiral PEPS and different environment dimension χ (as shown in legends) on semilog and log-log (inset) plots. The dashed (red) curve is a power-law $d^{-\alpha}$ fit. (b) Correlation lengths obtained from the fits of the long-distance correlations, shown vs χ/D^2, for both model parameter sets.

the fits are found to diverge linearly with χ, for both models studied, as shown in Fig. 5(b). At short distance, the data are better fitted as a power law $d^{-\alpha}$, although with a large exponent $\alpha \simeq 4.5$, rather than as an exponential. Thus, the power-law behavior takes over at all distances when $\chi \to \infty$. This suggests a form of emerging $U(1)$-gauge symmetry typical of dimer liquids [55] or RVB states [56–59] on bipartite lattices.

Summary and outlook. Using a previous symmetry classification of SU(2)-invariant PEPS we have constructed simple families of chiral PEPS on the square lattice. Using iPEPS supplemented by a CG algorithm, we have optimized these PEPS with respect to the local chiral (frustrated) AFHM, believed to host a CSL phase of the same class as the $\nu = \frac{1}{2}$ bosonic FQH liquid. The energy optimizations reveal very competitive *Ansätze* (better than the KL *Ansatz*) even for small bond dimensions $D = 3$ or $D = 4$. As expected in such a CSL phase, we find clear evidence of $SU(2)_1$ chiral edge modes. However, bulk properties turned out to have fundamental differences compared to a FQH gapped liquid: Although spin-spin and dimer-dimer correlations seem qualitatively different, both seem to reveal long-range behaviors. Although detailed data have been provided for two particular points in parameter space, a similar behavior has also been found between those two points. We conjecture that this may well be realistic features of the GS of (1) which would host in fact a *critical* CSL. Certainly, this does not contradict the results of Ref. [22] showing that, on small clusters, the KL state is an extremely good *Ansatz* for (1). Indeed, the short-range properties of our critical chiral PEPS are also likely to be extremely close to those of the KL state so that only the long-distance properties can distinguish them. Interestingly, it was proved that any strictly short-range quadratic parent Hamiltonian for chiral *free* fermions is gapless [36]. It may well be that this extends to interacting local Hamiltonians, in agreement with our findings. This would also agree with the fact that the CFT wave function derived using the null vectors of $SU(2)_1$ [22,29], i.e., the KL state, has a parent H that is long range.

Acknowledgments. This project is supported by the TNSTRONG ANR grant (French Research Council). This work was granted access to the HPC resources of CALMIP supercomputing center under the allocation 2017-P1231. I acknowledge inspiring conversations with Fabien Alet, Sylvain Capponi, Ignacio Cirac, Matthieu Mambrini, Anne Nielsen, Pierre Pujol, German Sierra, and Norbert Schuch. I am also grateful to Anne Nielsen for providing the variational energy of the KL state to compare to.

[1] X. G. Wen, Topological orders in rigid states, Int. J. Mod. Phys. B **04**, 239 (1990).

[2] X.-G. Wen, Topological order: From long-range entangled quantum matter to a unified origin of light and electrons, ISRN Condens. Matter Phys. **2013**, 198710 (2013).

[3] A. Yu. Kitaev, Fault-tolerant quantum computation by anyons, Ann. Phys. **303**, 2 (2003).

[4] H. L. Stormer and D. C. Tsui, The quantized Hall effect, Science **220**, 1241 (1983).

[5] R. B. Laughlin, Anomalous Quantum Hall Effect: An Incompressible Quantum Fluid with Fractionally Charged Excitations, Phys. Rev. Lett. **50**, 1395 (1983).

[6] G. Moore and N. Read, Nonabelions in the fractional quantum Hall effect, Nucl. Phys. B **360**, 362 (1991).

[7] N. Read and E. Rezayi, Beyond paired quantum Hall states: Parafermions and incompressible states in the first excited Landau level, Phys. Rev. B **59**, 8084 (1999).

[8] C. Repellin, T. Neupert, B. A. Bernevig, and N. Regnault, Projective construction of the $\mathbb{Z}_k$ Read-Rezayi fractional quantum Hall states and their excitations on the torus geometry, Phys. Rev. B **92**, 115128 (2015).

[9] B. I. Halperin, Statistics of Quasiparticles and the Hierarchy of Fractional Quantized Hall States, Phys. Rev. Lett. **52**, 1583 (1984).

[10] X. G. Wen, Non-Abelian Statistics in the Fractional Quantum Hall States, Phys. Rev. Lett. **66**, 802 (1991).

[11] X. G. Wen, Gapless boundary excitations in the quantum Hall states and in the chiral spin states, Phys. Rev. B **43**, 11025 (1991).

[12] X.-G. Wen, Theory of the edge states in fractional quantum Hall effects, Int. J. Mod. Phys. B **06**, 1711 (1992).

[13] P. Ginspary, Applied conformal field theory, in *Fields, Strings and Critical Phenomena*, edited by E. Brézin and J. Zinn-Justin, Proceedings of the Les Houches Summer School of Theoretical Physics, XLIX, 1988 (North-Holland, Amsterdam, 1988).

[14] B. Estienne, Z. Papić, N. Regnault, and B. A. Bernevig, Matrix product states for trial quantum Hall states, Phys. Rev. B **87**, 161112 (2013).

[15] B. Estienne, N. Regnault, and B. A. Bernevig, Correlation Lengths and Topological Entanglement Entropies of Unitary and Nonunitary Fractional Quantum Hall Wave Functions, Phys. Rev. Lett. **114**, 186801 (2015).

[16] V. Kalmeyer and R. B. Laughlin, Equivalence of the Resonating-Valence-Bond and Fractional Quantum Hall States, Phys. Rev. Lett. **59**, 2095 (1987).

[17] X. G. Wen, F. Wilczek, and A. Zee, Chiral spin states and superconductivity, Phys. Rev. B **39**, 11413 (1989).

[18] P. W. Anderson, Resonating valence bonds: A new kind of insulator? Mater. Res. Bull. **8**, 153 (1973).

[19] M. Levin and A. Stern, Fractional Topological Insulators, Phys. Rev. Lett. **103**, 196803 (2009).

[20] C. Repellin, B. A. Bernevig, and N. Regnault, $\mathbb{Z}_2$ fractional topological insulators in two dimensions, Phys. Rev. B **90**, 245401 (2014).

[21] J. Maciejko and G. A. Fiete, Fractionalized topological insulators, Nat. Phys. **11**, 385 (2015).

[22] A. E. B. Nielsen, G. Sierra, and J. I. Cirac, Local models of fractional quantum Hall states in lattices and physical implementation, Nat. Commun. **4**, 2864 (2013).

[23] B. Bauer, L. Cincio, B. P. Keller, M. Dolfi, G. Vidal, S. Trebst, and A. W. W. Ludwig, Chiral spin liquid and emergent anyons in a kagome lattice Mott insulator, Nat. Commun. **5**, 5137 (2014).

[24] D. F. Schroeter, E. Kapit, R. Thomale, and M. Greiter, Spin Hamiltonian for which the Chiral Spin Liquid is the Exact Ground State, Phys. Rev. Lett. **99**, 097202 (2007).

[25] R. Thomale, E. Kapit, D. F. Schroeter, and M. Greiter, Parent Hamiltonian for the chiral spin liquid, Phys. Rev. B **80**, 104406 (2009).

[26] M. Greiter, D. F. Schroeter, and R. Thomale, Parent Hamiltonian for the non-Abelian chiral spin liquid, Phys. Rev. B **89**, 165125 (2014).

[27] I. Glasser, J. I. Cirac, G. Sierra, and A. E. B. Nielsen, Exact parent Hamiltonians of bosonic and fermionic Moore-Read states on lattices and local models, New J. Phys. **17**, 082001 (2015).

[28] A. E. B. Nielsen, J. I. Cirac, and G. Sierra, Quantum spin Hamiltonians for the $SU(2)_k$ WZW model, J. Stat. Mech. (2011) P11014.

[29] A. E. B. Nielsen, J. I. Cirac, and G. Sierra, Laughlin Spin-Liquid States on Lattices Obtained from Conformal Field Theory, Phys. Rev. Lett. **108**, 257206 (2012).

[30] A. E. B. Nielsen, G. Sierra, and J. I. Cirac, Optical-lattice implementation scheme of a bosonic topological model with fermionic atoms, Phys. Rev. A **90**, 013606 (2014).

[31] J. I. Cirac and F. Verstraete, Renormalization and tensor product states in spin chains and lattices, J. Phys. A: Math. Theor. **42**, 504004 (2009).

[32] J. I. Cirac, Entanglement in many-body quantum systems, in *Many-Body Physics with Ultracold Atoms*, edited by C. Salomon, G. Shlyapnikov, and L. F. Cugliandolo, Lecture Notes of the Les Houches Summer School, XCIV, 2010 (Oxford University Press, Oxford, UK, 2010).

[33] R. Orús, A practical introduction to tensor networks: Matrix product states and projected entangled pair states, Ann. Phys. **349**, 117 (2014).

[34] N. Schuch, Condensed matter applications of entanglement theory, in *Quantum Information Processing: Lecture Notes of the 44th IFF Spring School 2013*, edited by D. P. DiVincenzo, Schriften des Forschungszentrums Jülich. Reihe Schlüsseltechnologien/Key Technologies Vol. 52 (Forschungszentrum Jülich, 2013), p. 29.

[35] R. Orús, Advances on tensor network theory: Symmetries, fermions, entanglement, and holography, Eur. Phys. J. B **87**, 1 (2014).

[36] J. Dubail and N. Read, Tensor network trial states for chiral topological phases in two dimensions and a no-go theorem in any dimension, Phys. Rev. B **92**, 205307 (2015).

[37] S. Yang, T. B. Wahl, H.-H. Tu, N. Schuch, and J. I. Cirac, Chiral Projected Entangled-Pair State with Topological Order, Phys. Rev. Lett. **114**, 106803 (2015).

[38] D. Poilblanc, J. I. Cirac, and N. Schuch, Chiral topological spin liquids with projected entangled pair states, Phys. Rev. B **91**, 224431 (2015).

[39] D. Poilblanc, N. Schuch, and I. Affleck, $SU(2)_1$ chiral edge modes of a critical spin liquid, Phys. Rev. B **93**, 174414 (2016).

[40] M. Mambrini, R. Orús, and D. Poilblanc, Systematic construction of spin liquids on the square lattice from tensor networks with SU(2) symmetry, Phys. Rev. B **94**, 205124 (2016).

[41] D. Poilblanc and M. Mambrini, Quantum critical phase with infinite projected entangled paired states, Phys. Rev. B **96**, 014414 (2017).

[42] T. Nishino and K. Okunishi, Corner transfer matrix renormalization group method, J. Phys. Soc. Jpn. **65**, 891 (1996).

[43] T. Nishino, Y. Hieida, K. Okunishi, N. Maeshima, Y. Akutsu, and A. Gendiar, Two-dimensional tensor product variational formulation, Prog. Theor. Phys. **105**, 409 (2001).

[44] R. Orús and G. Vidal, Simulation of two-dimensional quantum systems on an infinite lattice revisited: Corner transfer matrix for tensor contraction, Phys. Rev. B **80**, 094403 (2009).

[45] R. Orús, Exploring corner transfer matrices and corner tensors for the classical simulation of quantum lattice systems, Phys. Rev. B **85**, 205117 (2012).

[46] P. Corboz, Variational optimization with infinite projected entangled-pair states, Phys. Rev. B **94**, 035133 (2016).

[47] L. Vanderstraeten, J. Haegeman, P. Corboz, and F. Verstraete, Gradient methods for variational optimization of projected entangled-pair states, Phys. Rev. B **94**, 155123 (2016).

[48] W.-Y. Liu, S.-J. Dong, Y.-J. Han, G.-C. Guo, and L. He, Gradient optimization of finite projected entangled pair states, Phys. Rev. B **95**, 195154 (2017).

[49] W. H. Press, S. A. Teukolsky, W. P. Vetterling, and B. P. Flannery, *Numerical Recipes* (Cambridge University Press, Cambridge, UK, 2007).

[50] J. I. Cirac, D. Poilblanc, N. Schuch, and F. Verstraete, Entanglement spectrum and boundary theories with projected entangled-pair states, Phys. Rev. B **83**, 245134 (2011).

[51] H. Li and F. D. M. Haldane, Entanglement Spectrum as a Generalization of Entanglement Entropy: Identification of Topological Order in Non-Abelian Fractional Quantum Hall Effect States, Phys. Rev. Lett. **101**, 010504 (2008).

[52] J. Dubail, N. Read, and E. H. Rezayi, Real-space entanglement spectrum of quantum Hall systems, Phys. Rev. B **85**, 115321 (2012).

[53] J. Dubail, N. Read, and E. H. Rezayi, Edge-state inner products and real-space entanglement spectrum of trial quantum Hall states, Phys. Rev. B **86**, 245310 (2012).

[54] B. Herwerth, G. Sierra, H.-H. Tu, J. I. Cirac, and A. E. B. Nielsen, Edge states for the Kalmeyer-Laughlin wave function, Phys. Rev. B **92**, 245111 (2015).

[55] D. S. Rokhsar and S. A. Kivelson, Superconductivity and the Quantum Hard-Core Dimer Gas, Phys. Rev. Lett. **61**, 2376 (1988).

[56] A. F. Albuquerque and F. Alet, Critical correlations for short-range valence-bond wave functions on the square lattice, Phys. Rev. B **82**, 180408(R) (2010).

[57] Y. Tang, A. W. Sandvik, and C. L. Henley, Properties of resonating-valence-bond spin liquids and critical dimer models, Phys. Rev. B **84**, 174427 (2011).

[58] D. Poilblanc, N. Schuch, D. Pérez-García, and J. I. Cirac, Topological and entanglement properties of resonating valence bond wave functions, Phys. Rev. B **86**, 014404 (2012).

[59] N. Schuch, D. Poilblanc, J. I. Cirac, and D. Pérez-García, Resonating valence bond states in the PEPS formalism, Phys. Rev. B **86**, 115108 (2012).